Shaking table test and dynamic response analysis of reinforced concrete structure

H. Zhang & H.N. Li
Dalian University of Technology, P. R. China

B. Shang
Tsinghua University, P. R. China

SUMMARY:
As well known, reinforced concrete structures are often affected by dynamic loads such as earthquake ground motion, wind, blast and so on. The ultimate strength and initial elastic stiffness of concrete are increase, and behaviors of steel materials are obvious enhancement of yield stress with strain rate effect. However, few studies about nonlinear seismic response analysis of reinforced concrete structure consider the strain rate. A 1/5-scale three-story reinforced concrete frame-wall model was conducted on the shaking table. The tested results were used to verify the accuracy of nonlinear seismic analysis. The tested model was established in the finite element software ABAQUS. The beams and columns of the model were simulated by proposed fiber beam element, and shear wall was simulated by shell element. Results show that tested and calculated results were match well. The strain rate effect should be considered properly in nonlinear seismic analysis of reinforced concrete structures.

Keywords: Reinforced concrete structures, strain rate effect, dynamic behaviour, shaking table, nonlinear seismic analysis.

1. INTRODUCTION

The reinforced concrete structures are required to resist dynamic loads when subjected to seismic loading. The mechanical and deformation properties of reinforcing steel bar and concrete are rate dependent under the dynamic loads. The strain rate effect of concrete was firstly reported by Abrams in 1917 (Abrams 1917), analytical and experimental results presented by numerous investigators over the past few decades. The mechanical properties of the concrete and reinforcing steel bar were studied, among others, by (Fu et al. 1991), (Bischoff et al. 1991), (Cowell 1969) and (Wakabayashi et al. 1980). The strain rates of concrete and reinforcing steel bar constitute a ranging from 10^{-1} to 10^{-4} under the seismic loading. The strain rate of the concrete under a severe earthquake is about 10^{-2}/s, at this rate the strength of the concrete will be increased 1.2 times on the basis of the previous investigations (Shimazaki et al. 1998). The strain rate of the reinforcing steel bar is about 10^{-1}/s (Li et al. 2010), and the yield strength will be increased more. Hence, the strength, stiffness and ductility of the reinforced concrete structures will be influenced by the strain rate effect of the building materials. Since the mechanical properties of concrete and reinforcing steel bars are function of strain rate, a seismic response analysis of which considers the strain rate effect is more accurate. However, investigations on seismic response analysis that considers the strain rate effect have seldom been reported, because it is difficult to make the analytical model and to perform the mathematical calculations.

In this paper, a 1/5 scale reinforced concrete (RC) frame-wall model of shaking table was conducted to study the dynamic behavior and damage features of reinforced concrete structure under earthquake excitations which can also verify the accuracy of nonlinear seismic response analysis with strain rate effect. A finite element model of RC frame-wall structure in the shaking table test was also established in the finite element software ABAQUS. Based on finite element method (FEM), the dynamic fiber beam element with strain rate effect for beam and column was proposed. Shear wall was simulated by shell element. The proposed model can calculate the nonlinear seismic response of reinforced concrete structures under earthquakes.

2. SHAKING TABLE TEST OF RC RAME-WALL STRUCTURE

2.1. Description of model

The model was constructed in Dalian University of Technology (DUT) in China. As is shown in Figure 2.1, It was a 1/5-scale three-story reduced RC frame-wall model casted by micro-concrete (coarse aggregate size ≤5mm and properties are similar to concrete for reduced RC model in shaking table test) by considering the limit size of the shaking table 3m×4m and maximum loading capacity of 10t. The dimension of the model is shown in Figure 2.2. The main reinforcing steel in columns and beams were 3mm galvanized wires. The 2mm galvanized wire mesh was used as the reinforcing steel in two orthogonal directions in the walls and slabs. The ϕ0.9 iron wires were adopted for stirrups in the beams and columns.

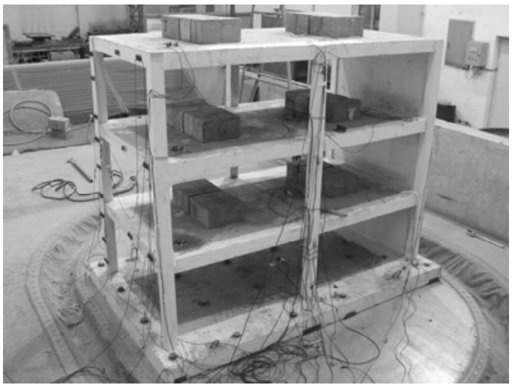

Figure 2.1. RC frame-wall model

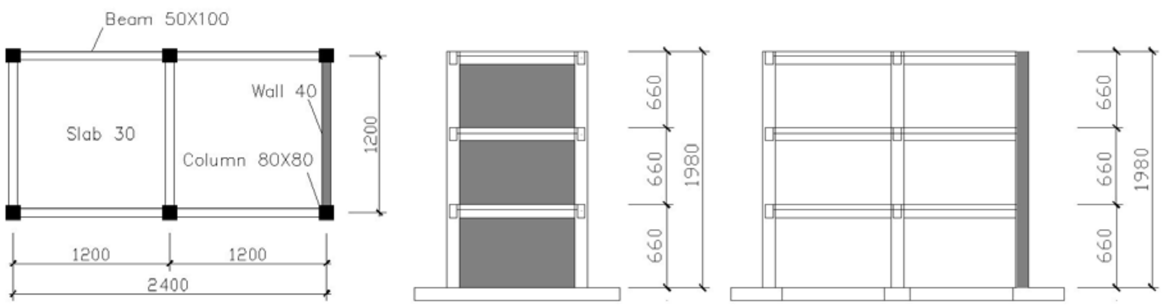

Figure 2.2. Dimension of model (unit: mm)

2.2. Similarity coefficient

In order to satisfy the similarity between the prototype structure and tested model in shaking table test, the artificial mass method is usually used. Thus, the sufficient artificial mass model was applied in the test. The additional weight was applied on the slabs by using the concrete blocks. Based on the sufficient artificial mass model (Zhang, 1997), the similarity coefficients are shown in Table 2.1.

2.3. Input motion and instrumentation

The typical ground motion El Centro wave (N-S component and vertical component) was selected as the input motion, that the maximum accelerations were 341.7cm/s^2 and 206.3cm/s^2, as is shown in Figure 2.3. The time interval of the records was compressed according to similarity coefficient of time.

The input peak ground acceleration of principal direction is shown in Table 2.2, and the vertical input motion was compressed according to the real ratio of the ground motion.

Table 2.1. Similarity coefficients of model

Physical quantity	Similarity relationship	Coefficient
Length	l_r	0.2
Elastic modulus	E_r	0.25
Equivalent density	$\overline{\rho_r} = \dfrac{m_m + m_a + m_{om}}{l_r^3(m_p + m_{op})}$	1.26
Stress	$\sigma_r = E_r$	0.25
Deflection	$r_r = l_r$	0.2
Time	$t_r = l_r / \sqrt{E_r / \overline{\rho_r}}$	0.447
Velocity	$v_r = \sqrt{E_r / \overline{\rho_r}}$	0.44
Acceleration	$a_r = E_r / (l_r \overline{\rho_r})$	1
Frequency	$\omega_r = \sqrt{E_r / \rho_r} / l_r$	2.237

Table 2.2. Test program

Test No.	Input PGA of principal direction (g)	Direction
WN-1	0.05	x
EC-1	0.16	x/z
EC-2	0.24	x/z
EC-3	0.33	x/z
EC-4	0.40	x/z
EC-5	0.45	x/z
EC-6	0.50	x/z
EC-7	0.54	x/z
EC-8	0.58	x/z
EC-9	0.60	x/z
EC-10	0.66	x/z
EC-11	0.70	x/z
EC-12	0.73	x/z
EC-13	0.86	x/z

Note: WN and EC denote White noise and El Centro records, respectively. PGA is peak ground

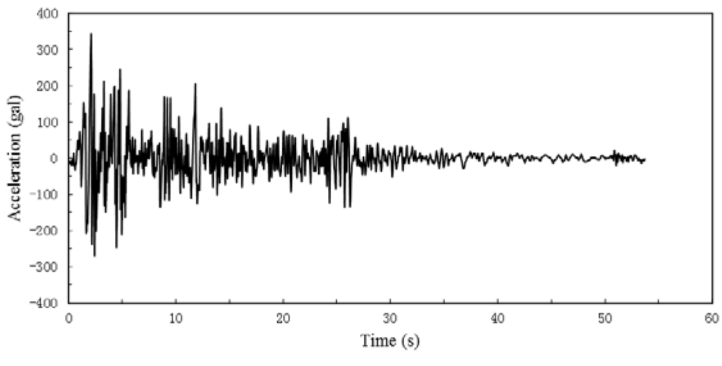

(a) N-S component

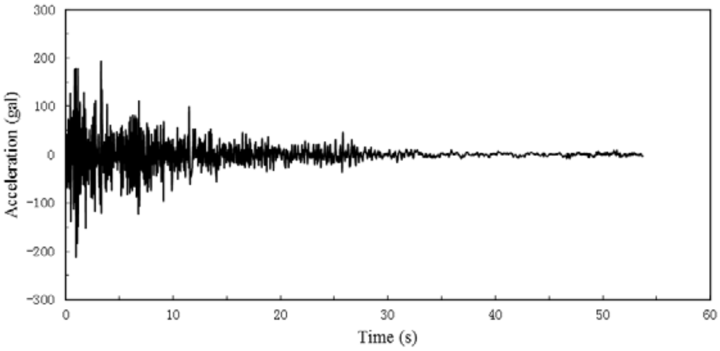

(b) Vertical component

Figure 2.3. El-Centro wave

Seventeen accelerometers and fifteen fiber optic sensors were applied on the tested model. The accelerometers (Figure 2.4) were fixed on the slabs, which were used to obtain the horizontal and vertical accelerations.

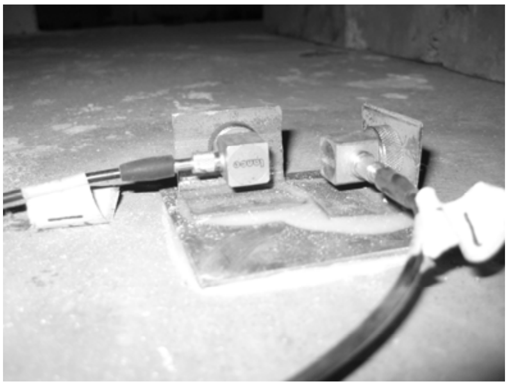

Figure 2.4. Accelerotransducer

2.4. Analysis of tested results

The effective frequencies and damping ratio which were obtained from the Fourier spectra of the roof acceleration time history are shown in Figure 2.5 and Figure 2.6. The frequency decreases and damping increases as the model damage progresses. The maximum responses of model are shown in Table 2.3.

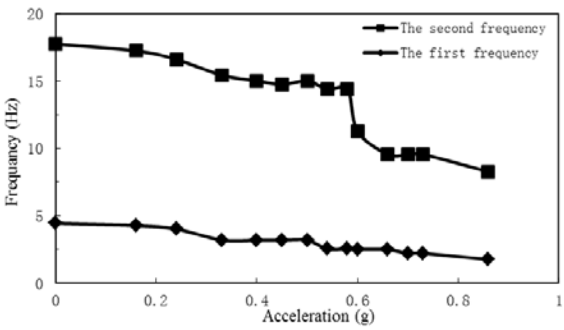

Figure 2.5. Effective frequencies

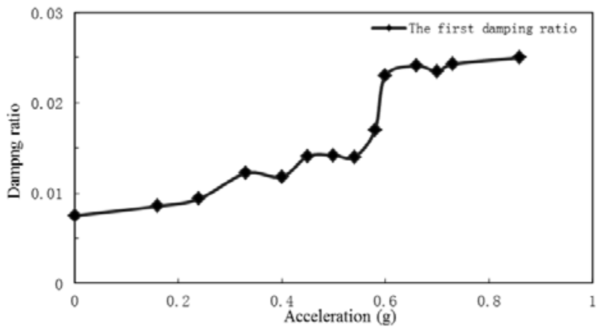

Figure 2.6. Damping ratio

Table 2.3. Maximum response of model

Input PGA of principal direction (g)	Horizontal direction			Vertical direction		
	Acceleration (g)	Displacement (cm)	Torsion (rad)	Acceleration (g)	Displacement (cm)	Torsion (rad)
0.16	0.274	0.273	0.00239	0.116	0.046	-
0.24	0.413	0.402	0.00338	0.232	0.051	-
0.33	0.452	0.536	0.00451	0.363	0.054	-
0.40	0.565	0.596	0.00496	0.524	0.057	-
0.45	0.649	0.714	0.00578	0.608	0.063	-
0.50	0.692	0.793	0.00698	0.609	0.067	-
0.54	0.709	0.906	0.00797	0.624	0.073	-
0.58	0.756	1.051	0.00918	0.726	0.098	-
0.60	0.781	1.158	0.01035	0.829	0.106	-
0.66	0.848	1.351	0.01224	0.955	0.146	-
0.70	0.947	1.796	0.01573	1.140	0.164	-
0.73	0.839	2.475	0.02222	1.285	0.184	-
0.86	1.247	2.664	0.02394	1.770	0.265	-

3. FIBER BEAM ELEMENT MODEL

The proposed fiber beam element is discretized into longitudinal concrete and steel fibers. The element is based on the assumption that plane section remain plane and small displacement and deformations during the loading history. The nonlinear behaviour of the element derives from the one dimensional nonlinear stress-strain relation of the concrete and steel fibers. The fiber beam element model was embedded into the finite elemnt software ABAQUS as the explicit user-defined dynamic material subroutine (VUMAT) for nonlinear time-history analysis. The element of concrete is developed with the hysteresis constitutive law of concrete depending on the Code for design of concrete structures (GB 50010-2010). The uniaxial stress-strain curves of concrete are shown in Figure 3.1.

Uniaxial tensile stress strain relationship of concrete

$$\sigma = (1 - d_t) E_c \varepsilon \tag{3.1}$$

$x \leqslant 1$

$$d_t = 1 - \rho_t [1.2 - 0.2x^5] \tag{3.2}$$

$x > 1$

$$d_t = 1 - \frac{\rho_t}{\alpha_t (x-1)^{1.7} + x} \tag{3.3}$$

$$x = \frac{\varepsilon}{\varepsilon_{t,r}} \tag{3.4}$$

$$\rho_t = \frac{f_{t,r}}{E_c \varepsilon_{t,r}} \tag{3.5}$$

where α_t is the parameter of the descending portion in the uniaxial tensile stress strain curve. $f_{t,r}$ is the uniaxial compressive strength, $\varepsilon_{t,r}$ is the strain of peak stress. d_t is uniaxial tensile damage parameter. E_c is the elastic modulus.

Uniaxial compressive stress strain relationship of concrete

$$\sigma = (1 - d_c) E_c \varepsilon \tag{3.6}$$

$x \leqslant 1$

$$d_c = 1 - \frac{\rho_c n}{n - 1 + x^n} \tag{3.7}$$

$x > 1$

$$d_c = 1 - \frac{\rho_c}{\alpha_c (x-1)^2 + x} \tag{3.8}$$

$$\rho_c = \frac{f_{c,r}}{E_c \varepsilon_{c,r}} \tag{3.9}$$

$$n = \frac{E_c \varepsilon_{c,r}}{E_c \varepsilon_{c,r} - f_{c,r}} \tag{3.10}$$

$$x = \frac{\varepsilon}{\varepsilon_{c,r}} \tag{3.11}$$

where α_c is the parameter of the descending portion in the uniaxial compressive stress strain curve. $f_{c,r}$ is the uniaxial compressive strength, $\varepsilon_{c,r}$ is the strain of peak stress. d_c is uniaxil compressive damage parameter.

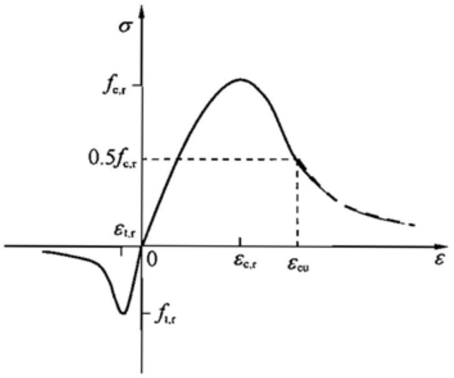

Figure 3.1. The uniaxial stress-strain curves of concrete

As is shown in Figure 3.2, the loading and unloading path of concrete under repeated loading was obtained from Eq. 3.12 to 3.15.

$$\sigma = E_r (\varepsilon - \varepsilon_z) \tag{3.12}$$

$$E_r = \frac{\sigma_{un}}{\varepsilon_{un} - \varepsilon_z} \tag{3.13}$$

$$\varepsilon_z = \varepsilon_{un} - (\frac{(\varepsilon_{un} + \varepsilon_{ca})\sigma_{un}}{\sigma_{un} + E_c\varepsilon_{ca}}) \tag{3.14}$$

$$\varepsilon_{ca} = \max(\frac{\varepsilon_c}{\varepsilon_c + \varepsilon_{un}}, \frac{0.09\varepsilon_{un}}{\varepsilon_c})\sqrt{\varepsilon_c\varepsilon_{un}} \tag{3.15}$$

where σ_c is the compressive strength of concrete, ε is the strain of concrete. ε_z is the residual strain of concrete. E_r is the modulus of the unloading reloading. σ_{un} and ε_{un} are the stress and strain at the beginning of unloading. ε_{ca} is the additional strain of concrete. ε_c is the peak value strain of concrete.

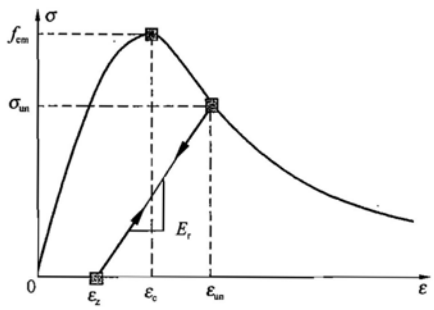

Figure 3.2. The stress strain curve of concrete under repeated loading

For steel element, bilinear kinematic hardening model was used to simulate the behaviors of yielding, hardening and Bauschinger's effect. The slope of plastic stage is 0.01Es.

4. NONLINEAR SEISMIC RESPONSE ANALYSIS WITH STRAIN RATE EFFECT

The shaking table test of section two in this paper was simulated with the proposed fiber beam element model. The finite element model was established in the finite element software ABAQUS which is shown in Figure 4.1. The beams and columns of model were modeled by the proposed fiber beam element, and the slabs and shear walls were modeled by shell element.

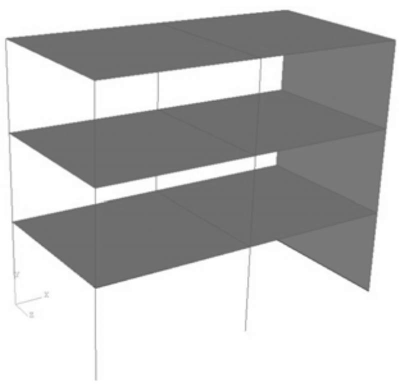

Figure 4.1. Finite element model in shaking table test

4.1 Modal analysis

In order to verify the accuracy of the finite element model, modal analysis was executed in ABAQUS. The first three vibration modes of model were shown in Figure 4.2. The first natural frequency obtained from modal analysis is 4.407Hz which is closed to the experimental result 4.425Hz. Hence, the finite element model has the similar dynamic behaviour with the tested model.

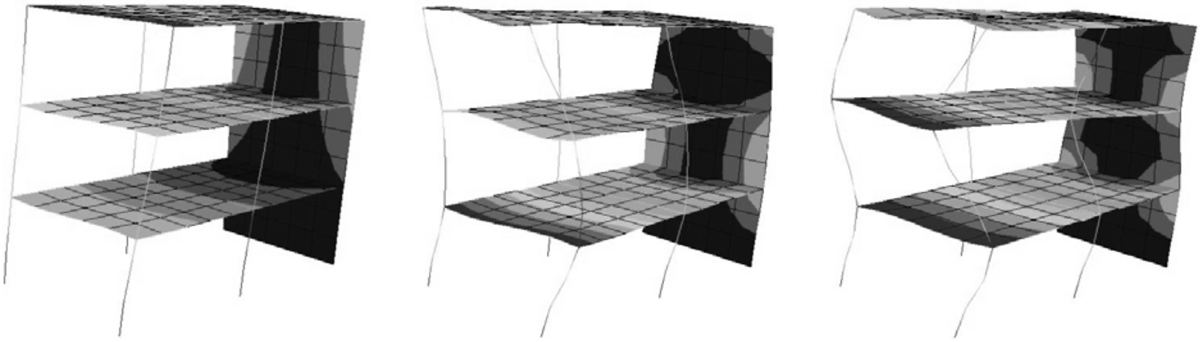

(a) First vibration mode 4.407Hz (b) Second vibration mode 14.132Hz (c) Third vibration mode 24.414Hz

Figure 4.2. Vibration modes

4.2 Constitutive models of concrete and steel with strain rate

The reduced reinforced concrete models are often casted by micro-concrete instead of concrete in shaking table test. The reinforcing steel in the beams and columns are also replaced by galvanized wires. Hence, the dynamic constitutive models of micro-concrete and galvanized wire (Zhang, 2012) obtained from the dynamic loading test under seismic strain rate are used in the proposed fiber beam element to calculate nonlinear seismic response of reduced reinforced concrete models. Eq. 4.1 is the relationship between compressive strength increment and strain rate of micro-concrete.

$$f_c^d / f_c^s = 0.9892 + 0.08607 \lg(\dot{\varepsilon}_d / \dot{\varepsilon}_s) \quad (4.1)$$

where f_c^d is the dynamic ultimate compressive strength of micro-concrete, f_c^s is the ultimate compressive strength of micro-concrete under quasi-static stain rate, $\dot{\varepsilon}_d$ is the strain rate, $\dot{\varepsilon}_s$ =10^{-5}/s is quasi-static stain rate.

For the dynamic tensile constitutive model of micro-concrete, studies about the dynamic tensile constitutive model of micro-concrete have not seen at present. The dynamic tensile constitutive model of micro-concrete is approximately replaced by the model of lower strength concrete (Yan, 2006). Eq. 4.2 is the relationship between tensile strength increment and strain rate of micro-concrete.

$$DIF = 1.0 + 0.135 \lg(\dot{\varepsilon}_t / \dot{\varepsilon}_{ts}) \quad (4.2)$$

where DIF is the ratio of dynamic tensile strength to static tensile strength, $\dot{\varepsilon}_t$ is the strain rate, $\dot{\varepsilon}_{ts}$ =10^{-5}/s is quasi-static stain rate.

For galvanized wire, Eq. 4.3 and Eq. 4.4 are yield strength and tensile strength increment which are function of strain rate, respectively.

$$\frac{f_{yd}}{f_{ys}} = 1.0 + 0.0456 \lg\left(\frac{\dot{\varepsilon}_w}{\dot{\varepsilon}_{w0}}\right) \quad (4.3)$$

$$\frac{f_{ud}}{f_{us}} = 1.0 + 0.0212 \lg\left(\frac{\dot{\varepsilon}_w}{\dot{\varepsilon}_{w0}}\right) \quad (4.4)$$

where $\dot{\varepsilon}_w$ is strain rate, $\dot{\varepsilon}_{w0}$ =2.5×10^{-4}/s is quasi-static stain rate, f_{ys} and f_{yd} are static and dynamic yield strength, f_{us} and f_{ud} are static and dynamic tensile strength.

4.3 Comparisons of numerical and experimental results

After EC-4 test the model had visible cracks and entered into plastic damage stage. The comparisons of numerical and tested results of EC-4 and EC-9 in horizontal direction are shown in Figure 4.3, Figure 4.4 and Figure 4.5. The numerical and tested results are match well which means the proposed fiber beam element can simulate the seismic performance of reinforced concrete structure accurately.

5. CONCLUSION

(1) Dynamic behavior and damage features of reinforced concrete structure under earthquake excitations were investigated by the shaking table test.
(2) The fiber beam element was proposed for nonlinear time-history analysis in which strain rate can take into account. The numerical results calculated by proposed model were match well with the experimental results.
(3) Strain rate effect should be considered properly in nonlinear time-history analysis.

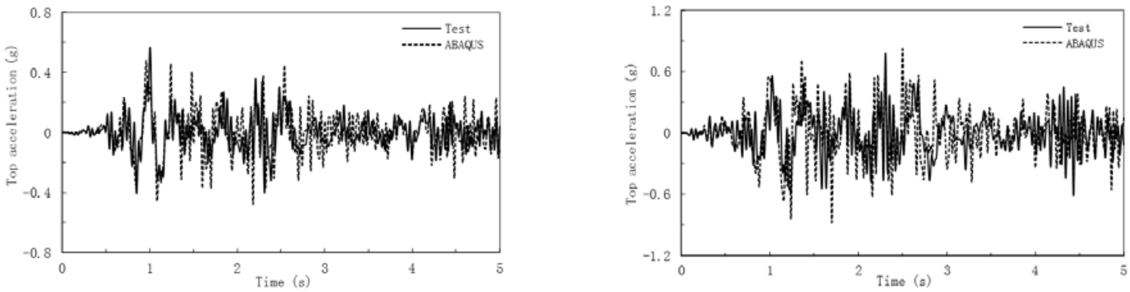

(a) 0.40g El Centro wave (b) 0.60g El Centro wave

Figure 4.3 Comparisons of numerical and experimental results of top acceleration time-histories in horizontal direction

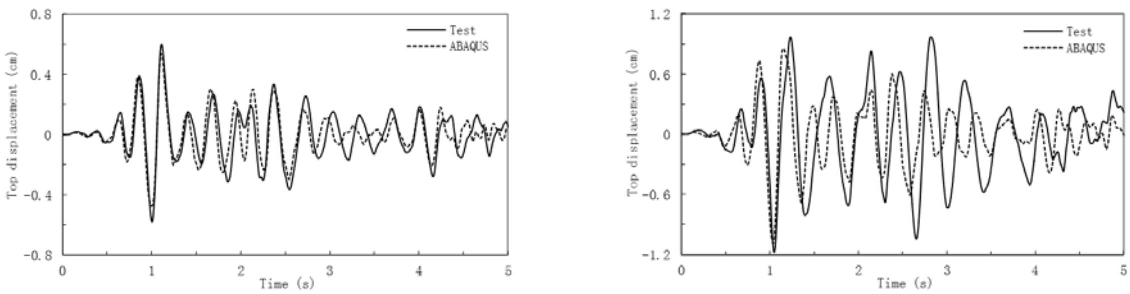

(a) 0.40g El Centro wave (b) 0.60g El Centro wave

Figure 4.4 Comparisons of numerical and experimental results of top displacement time-histories in horizontal direction

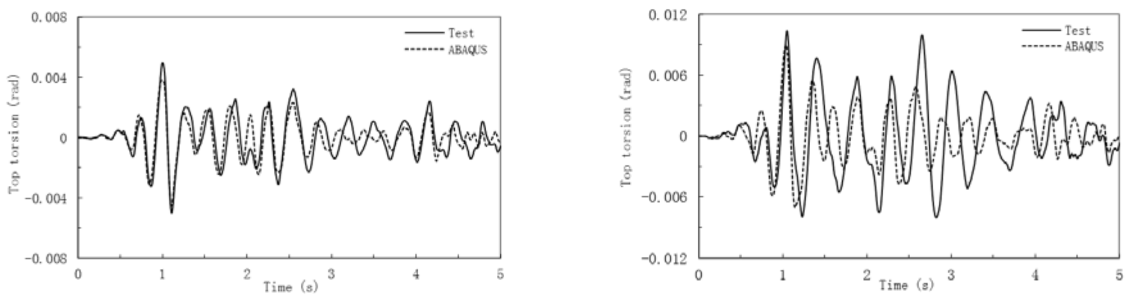

(a) 0.40g El Centro wave (b) 0.60g El Centro wave

Figure 4.5 Comparisons of numerical and experimental results of top torsional time-histories in horizontal direction

AKCNOWLEDGEMENT

This work was financially supported by the Major Program of National Natural Science Foundation of China (90815026).

REFERENCES

Abrams, D. A. (1917). Effect of rate of application of load on the compressive strength of concrete. *Proc., 20th Annu. Meeting, ASTM*. **Vol 17:** 366-374.

Fu, H. C., Seckin, M. and Erki, M. A. (1991). Review of effects of loading rate on reinforced concrete. *Journal of Structural Engineering (ASCE)* **117:12**,3660-3670.

Bischoff, P. H. and Perry, S. H. (1991). Compressive behaviour of concrete at high strain rates. *Materials and Structures* **24:6**,425-450.

Cowell, W. L. (1969). Dynamic tests on selected structural steels. *Tech. Rep. No. R642,* U.S. Naval Civil Engineering Lab., Port Hueneme, Calif.

Wakabayashi, M., Nakamura, T., Yoshida, N., Iwai, S. and Watanbe, Y. (1980). Dynamilc loading effects on structural performance of concrete and steel materials and beams. *Proc. Seventh World Conference on Earthquake Engineering.* **Vol 6:** 271-278.

Shimazaki, K. and Wada, A. (1998) Dynamic analysis of a reinforced concrete shear wall with strain rate effect. *ACI Structural Journal* **95:5,**488-497.

Li, M. and Li, H. N. (2010). Dynamic test and constitutive model for reinforcing steel bar. *China Civil Engineering Journal* **43:4,** 70-75.

Zhang, M. Z. (1997). Study on similitude laws for shaking table tests. *Earthquake Engineering and Engineering Vibration1***7:2,** 52-58.

GB 50010-2010 Code for design of concrete structures, China Architecture & Building Press, Beijing, China.

Zhang, H. (2012). Strain rate effect of materials on seismic response of reinforced concrete frame-wall structure，Dalian University of Technology, Dalian, China.

Yan, D. M. (2006). Experimental and theoretical study on the dynamic properties of concrete，Dalian University of Technology, Dalian, China.